

# On the Structure of Sulfur/1,3-Diisopropenylbenzene Co-Polymer Cathodes for Li-S Batteries: Insights from Density-Functional Theory Calculations

Rana Kiani,<sup>[a]</sup> Daniel Sebastiani,<sup>[a]</sup> and Pouya Partovi-Azar\*<sup>[a]</sup>

Sulfur co-polymers have recently drawn considerable attention as alternative cathode materials for lithium-sulfur batteries, thanks to their flexible atomic structure and the ability to provide high reversible capacity. Here, we report on the atomic structure of sulfur/1,3-diisopropenylbenzene co-polymers (poly(S-co-DIB)) based on the insights obtained from density-functional theory calculations. The focus is set on studying the local structural properties, namely the favorable sulfur chain length ( $S_n$  with  $n = 1 \cdots 8$ ) connecting two DIBs. In order to investigate the effects of the organic groups and sulfur chains separately, we perform series of atomic structure optimizations. We start from simple organic groups connected via sulfur chains and

gradually change the structure of the organic groups until we reach a structure in which two DIB molecules are attached via sulfur chains. Additionally, to increase the structural sampling, we perform temperature-assisted minimum-energy structure search on slightly simpler model systems. We find that in DIB- $S_n$ -DIB co-polymers, shorter sulfur chains with  $n \sim 4$  are preferred, where the stabilization is mostly brought about by the sulfur chains rather than the organic groups. The presented results, corresponding to the fully charged state of the cathode in the thermodynamic limit, have direct applications in the field of lithium-sulfur batteries with sulfur-polymer cathodes.

## 1. Introduction

With the ever growing global demand for energy, the quest for finding more efficient energy-storage systems has become more and more intensive. Recently, lithium-sulfur (Li-S) batteries have shown a superior performance over lithium-ion batteries in terms of the energy density.<sup>[1,2]</sup> Additionally, abundance of the constituents makes the Li-S a promising candidate for the next-generation energy-storage devices. However, irreversible capacity fade observed in the Li-S batteries through cycling have so far prevented them from being used in electric devices.<sup>[3]</sup> This is mainly due to the formation of Li-polysulfides during the discharge which could consume the active material and lead to a shuttle effect.<sup>[4,5]</sup> Another problem which has hindered the commercial production of the Li-S batteries is the volumetric expansion of the sulfur cathode upon lithiation which can detach the electrode from the current collectors and even bring about safety issues.<sup>[3,6,7]</sup>

In this regard, polymeric materials have been widely proposed and investigated as alternative cathodes for Li-S

batteries.<sup>[8–15]</sup> In particular, sulfur/carbon co-polymers, usually synthesized through an inverse vulcanization process, have recently attracted much attention.<sup>[9,16]</sup> As sulfur cathode materials, they are not only able to withstand the volumetric expansion of the cathode during discharge, thanks to their structural flexibility, but they also have demonstrated a promising performance in improving the cycle life of Li-S batteries. Recently, sulfur/1,3-diisopropenylbenzene co-polymers (poly(S-co-DIB)) have been shown to substantially immobilize the Li-polysulfides during lithiation of the cathode.<sup>[16,17]</sup> It has been shown that the improved cyclability stems from the organic moieties which act as anchors that fixate the Li-polysulfides to the polymeric network and, therefore, prevent them from diffusing into the electrolyte.<sup>[17]</sup> However, the redox mechanisms of these materials are still not fully known. This is due to the difficulty in characterizing amorphous polymer cathode structures and identifying individual ionic species.

In this work, with the aim to gather insights onto the structure of poly(S-co-DIB) co-polymers, we combine density-functional theory-based calculations together with classical molecular dynamics simulations to study the local bonding between DIB and sulfur chains. We aim at finding the most favorable length of a sulfur chain connecting two DIBs and further use these information to gather insights onto the bulk structure of the whole poly(S-co-DIB).

## 2. Methodology

A 1,3-diisopropenylbenzene (DIB) molecule is shown in Figure 1(a). Through the inverse vulcanization process to synthesize poly(S-co-DIB) co-polymers, the non-aromatic double C=C

[a] R. Kiani, Prof. Dr. D. Sebastiani, Dr. P. Partovi-Azar  
Institute of Chemistry, Martin-Luther-University Halle-Wittenberg  
Von-Danckelmann-Platz 4, 06120 Halle (Saale), Germany  
E-mail: pouya.partovi-azar@chemie.uni-halle.de

Supporting information for this article is available on the WWW under <https://doi.org/10.1002/cphc.202100519>

© 2021 The Authors. ChemPhysChem published by Wiley-VCH GmbH. This is an open access article under the terms of the Creative Commons Attribution Non-Commercial NoDerivs License, which permits use and distribution in any medium, provided the original work is properly cited, the use is non-commercial and no modifications or adaptations are made.

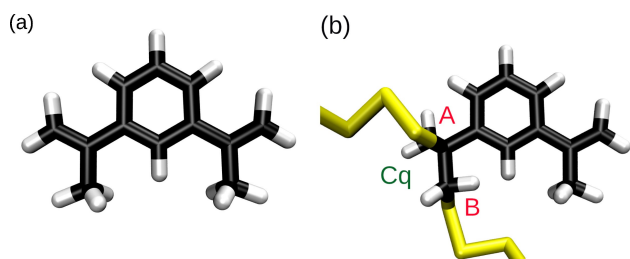
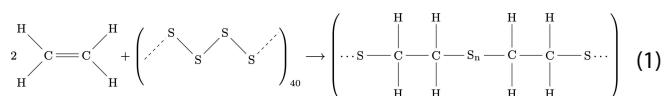


**Figure 1.** (a) A 1,3-diisopropenylbenzene molecule. (b) A local view of a poly(S-co-DIB) co-polymer during the inverse vulcanization process where two sulfur chains are connected to the organic moieties through a “quaternary” carbon  $C_q$  (connection A) and via  $CH_2$  group (connection B).

bonds almost completely turn into single bonds resulting in two  $sp^3$  hybridized carbon atoms (Figure 1(b)).<sup>[16]</sup>

To be able to gather insights into the structure of poly(S-co-DIB) co-polymers, we concentrate on their local structure with the aim to find the most favorable length of the sulfur chains which form the poly(S-co-DIB) network. There are two factors which play important roles in thermodynamic stabilization of the DIB- $S_n$ -DIB structures, namely the sulfur chain connecting the two DIBs and the interaction between the DIBs. In order to decompose these effects, first we start from a very simple compound as a product of the reaction 1 in which two  $C_2H_4$  molecules react with a polymeric sulfur chain consisting of a large number of sulfur atoms (here, 40 in total) with the terminal sulfur atoms saturated with hydrogen atoms to prevent radical effects.



We change  $n$  from 1 to 8 while keeping the total number of sulfur atoms constant. The large total number of sulfur atoms are considered here to avoid finite-size effects. Afterwards, chemical branches are gradually added to the two  $C_2H_4$  groups in the product structures until the structures of two DIBs are reached. To this end, first the hydrogen atoms bonded to C- $S_n$  are both replaced with a methyl group. In a next step, we replace the other hydrogens bonded to the same carbons with methyl groups as well. In next steps, two benzene rings are added to the structure and finally, the obtained structure is further modified to reach the target ( $\cdots$ S-DIB- $S_n$ -DIB- $S\cdots$ ),  $n = 1 \cdots 8$  structures. The above steps are schematically shown in Figure 2. In order to focus mainly on the effect of the additional carbon groups, at each step we start the structural optimization from the optimized structures obtained in the last step. Additionally, in order to further avoid the effects of structural flexibility of sulfur side chains we also perform structural optimizations under periodic boundary conditions.

All structural optimizations are carried out at density-functional theory (DFT) level using the CP2K software package.<sup>[18]</sup> A DZVP-MOLOPT basis set,<sup>[19]</sup> along with Perdew-Burke-Ernzerhof (PBE)<sup>[20,21]</sup> exchange-correlation energy functional and Geo-

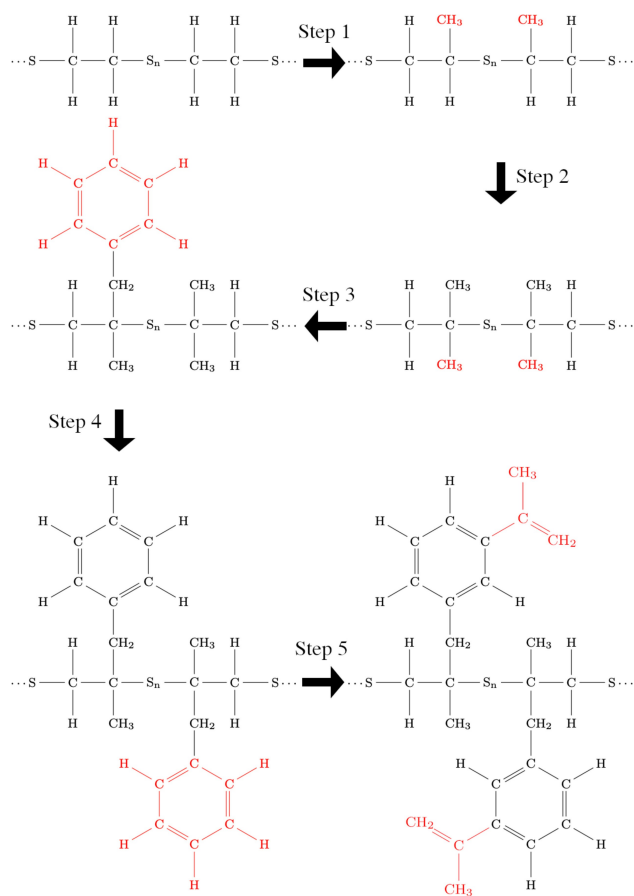


**Figure 2.** A schematic showing the steps taken in the present work from a simple ( $\cdots$ S- $CH_2$ - $CH_2$ - $S_n$ - $CH_2$ - $CH_2$ - $S\cdots$ ) structure to the final ( $\cdots$ S-DIB- $S_n$ -DIB- $S\cdots$ ) structure. The groups which are added at each step are highlighted in red.

decker-Teter-Hutter (GTH) pseudopotentials<sup>[22]</sup> are employed. Moreover, for the long-range dispersion interactions, the semi-empirical DFT-D3 method<sup>[23]</sup> is used. The synthesis of poly(S-co-DIB) co-polymers is a solvent-free process and the DIBs are added to the molten sulfur after ring-opening polymerization.<sup>[16]</sup> Therefore, all calculations in this work are performed in vacuum.

Moreover, to have a better structural sampling we adapt a temperature-assisted minimum-energy structure search on simpler structures consisting of two DIB molecules and a connecting S chain only, namely DIB- $S_n$ -DIB. The initial configurations are selected based on possible ways a sulfur chain can attach to two DIB molecules. There are two connection possibilities; (A) the S chain directly connects to the doubly bonded carbon, and (B) it connects to the DIB via a methyl group (Figure 1(b)). The former results in a carbon atom which is covalently bonded to four non-hydrogen atoms. Here, they are referred to as “quaternary” carbons,  $C_q$ , and are shown in Figure 1(b). As a result, three possible connections are considered, i.e.  $c = AA, AB, BB$ . In order to find candidates for the lowest-energy structure of DIB- $S_n$ -DIB,  $n = 1 \cdots 8$ , with different connections  $c$ , first for each  $(c, n)$  10 ns classical molecular

dynamics (MD) simulations at 300 K using General Amber Force Field (GAFF)<sup>[24]</sup> as implemented in the GULP code<sup>[25–27]</sup> are carried out. The atomic charges are calculated using the RESP method at DFT<sup>[28]</sup> level employing the sphere sampling of the fitting points for molecular structures<sup>[29]</sup> together with the REPEAT method.<sup>[30]</sup> A time step of 0.5 fs is considered in all simulations while the temperature is controlled using a Nosé-Hoover thermostat.<sup>[31,32]</sup> For each  $(c, n)$ , 10 uncorrelated snapshots are extracted from the MD trajectories roughly every 1 ns, resulting in total 240 sample structures. DFT-based geometry optimizations are then performed for all these structures.

### 3. Results and discussion

As mentioned above, in order to investigate how the sulfur chains and organic groups affect the total stability of poly(S-co-DIB) copolymers, we gradually change the organic moieties towards the target structure  $(\dots\text{S-DIB-S}_n\text{-DIB-S}\dots)$  (see Figure 2). The optimized structures and the respective DFT energies are shown in Figure 3(a)–(l) (the energies are referenced with respect to  $n = 4$  in all cases.) Here, we use the DFT energies since the entropic contribution to the free energy is found to be very small in the samples considered here (please see the SI). Figure 3(a) shows the lowest energy structure of  $\text{S}_{18}\text{-C}_2\text{H}_4\text{-S}_n\text{-C}_2\text{H}_4\text{-S}_{18}$  with  $n = 4$ . The total number of sulfur atoms in all samples in Figure 3 is constant (i.e. 40). Therefore, the total DFT energies can be directly considered as a stability measure. Here, the middle sulfur chains with  $n = 4, 8$  show the lowest energies. Explicit check for  $n = 9$  in the case of  $\text{S}_{18}\text{-C}_2\text{H}_4\text{-S}_n\text{-C}_2\text{H}_4\text{-S}_{18}$  reveals less favorable structures for longer middle chains with  $n > 8$ . To see whether  $n = 4, 8$  truly represent the most favorable number of sulfur atoms on the middle sulfur chain, we slightly modify the structures in the following way: while the total number of S atoms in the middle chain is kept fixed, the carbon groups from both sides are equally moved in one direction by several bonds. Afterwards, the structures are re-optimized. We see that in such a modification,

$n = 4$  still remains to be the most favorable number of S atoms for the middle chain. However, small structural changes around  $n = 8$  lead to structures with higher energies (please see the SI for more detail). The results in Figure 3 also indicate that the stability of the poly(S-co-DIB) is mainly brought about by the sulfur middle chains rather than the interaction between the organic groups. Therefore, although the interaction between the two DIBs could be different when different carbons engage in their connection to the middle sulfur chain (Figure 1(b)), as will be shown later, the local connection of the middle S chain to the DIBs could only play a minor role in specifying the length of the middle S chain,  $n$ .

To study electronic contributions to the thermodynamic stability of DIB-S<sub>n</sub>-DIB systems, we decompose the total energy of all  $(\dots\text{S-DIB-S}_n\text{-DIB-S}\dots)$  systems (Figure 3(k) and (l)) into nuclear and electronic parts. Our specific inspection reveals that, within the electronic part, only the exchange-correlation and the dispersion (also a correlation effect) contributions approximately follow the same trend as the total energy (see the SI). Therefore, we conclude that the electronic properties play an important role in the thermodynamic stability of the DIB-S<sub>n</sub>-DIB and these effects are mostly of quantum mechanical nature.

In a next step, in order to minimize the effects corresponding to the geometrical flexibility of sulfur side chains on the energies of the  $(\dots\text{S-DIB-S}_n\text{-DIB-S}\dots)$  structures, we consider periodic samples. An optimized structure for  $(\dots\text{S-DIB-S}_4\text{-DIB-S}\dots)$  is shown in Figure 4(a). The corresponding energies are presented in Figure 4(b). Here, we also study the possible effect of different connections between the middle sulfur chain and the DIBs, namely  $c = \text{AA}, \text{AB}, \text{and BB}$ . The unit cell size is set to  $30 \text{ \AA} \times 63 \text{ \AA} \times 30 \text{ \AA}$ , the structure lies along the  $y$ -axis, and each side chain consists of 22 sulfur atoms. The cell sides along the  $x$ - and  $z$ -axes together with the unit cell angles are kept fixed. They are long enough to ensure a negligible interaction between the atoms in the unit cell and those in the cell replicas. The cell size along  $y$ -axis was obtained after a full (atomic coordinates and cell parameters) optimization of an isolated

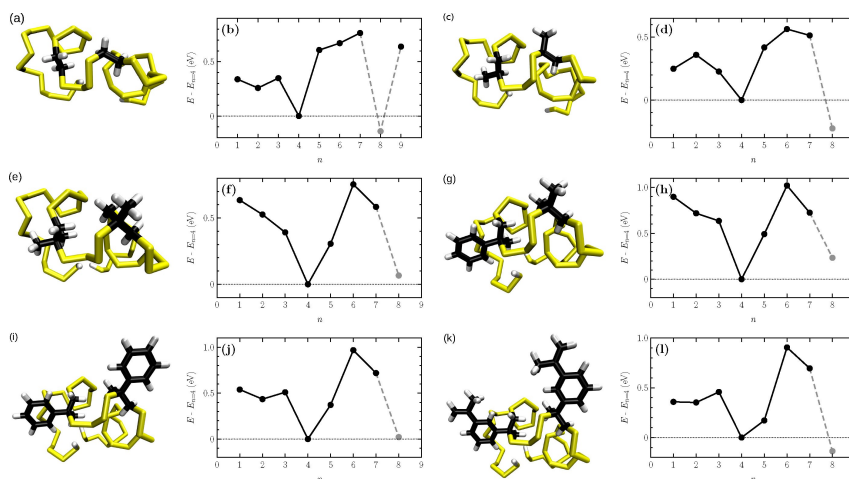


**Figure 3.** (a) Optimized structures of  $\text{S}_{18}\text{-C}_2\text{H}_4\text{-S}_n\text{-C}_2\text{H}_4\text{-S}_{18}$ ,  $n = 4$ . (b) Corresponding DFT energies for the optimized structures  $\text{S}_{18}\text{-C}_2\text{H}_4\text{-S}_n\text{-C}_2\text{H}_4\text{-S}_{18}$  with  $n = 1 \dots 8$ . The energies are referenced with respect to  $n = 4$  in all cases. (c)–(l) show the same for the optimized structures obtained by step-wise modifications shown in Figure 2. The gray circles show the energies for  $n = 8$  samples. However, these samples do not represent stable structures (see text).

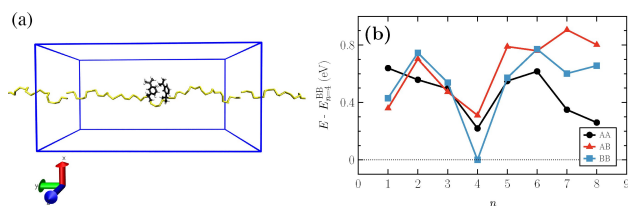
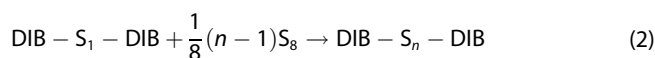


**Figure 4.** (a) The optimized periodic structure of  $(\dots\text{S-DIB-S}_n\text{-DIB-S}\dots)$  with 4 sulfur atoms in the middle chain. The unit cell is shown in blue. (b) DFT energies as a function of number of sulfur atoms in the middle chain,  $n$ . Data shown in black circles, red triangles, and blue squares correspond to AA, AB, and BB connections between the middle sulfur chain and the DIBs. The energies are referenced with respect to the energy of the sample with  $(c, n) = (\text{BB}, 4)$ .

sulfur chain consisting of 48 atoms. The target pressure was set to 0.1 GPa. As can be seen in Figure 4(b), the structures with  $n = 4$  again show lowest energies (apart from  $(c, n) = (\text{AA}, 8)$  which shows a comparable energy to  $(\text{AA}, 4)$ ). Additionally, different connections between the middle sulfur chain and the DIBs do not appear to have a considerable effect on the stability of the samples.  $n = 4$  approximately corresponds to a poly(S-co-DIB) network with an average DIB mass fraction of  $\sim 38$  wt%. This mass fractions nearly correspond to the S-DIB-40 samples studied in Refs. [16,17]. The predicted sulfur chain lengths in the present work perfectly match the experimental assignments using  $^{13}\text{C}$  NMR chemical shifts<sup>[17]</sup> and electrochemical measurements<sup>[16]</sup> ( $n \approx 3, 4$ ). Therefore, with the poly(S-co-DIB) co-polymers as cathode materials for Li-S batteries, the formation of higher-order Li-polysulfides could considerably be hindered during the discharge due to the preferred shorter sulfur chains in the cathode structure. In fact, this has been previously shown through electrochemical measurements that the poly(S-co-DIB) co-polymers with comparable DIB mass fraction exhibit an almost plateau-free voltage curve as a function of the state of discharge at high voltages.<sup>[16,17]</sup> However, low mass fraction of the active material could lead to a limited cathode capacity.

Finally, in order to enhance the structural sampling and further assess the results obtained from the geometry optimizations above, we perform a temperature-assisted minimum-energy structure search (for details see Sec. 2) on slightly simpler samples of DIB-S<sub>n</sub>-DIB without sulfur side chains. To this end, we consider the following hypothetical reaction,



which would correspond to a situation where an infinitely large reservoir of S<sub>8</sub> molecules with zero chemical potential is available for the DIB molecules. Moreover, here we also study the effect of different connections between the middle sulfur chain and the DIBs. Based on the above reaction, we define the formation energy per sulfur atom for each DIB-S<sub>n</sub>-DIB structures with a given connection  $c$ , as

$$E_{\text{form}}^{(c,n)} = \frac{1}{n} \left[ E_{\text{tot}}^{(c,n)} - \frac{1}{8}(n-1)E_{\text{tot}}^{(\text{S}_8)} - E_{\text{tot}}^{(c,1)} \right], \quad (3)$$

where  $E_{\text{tot}}$  denotes the total DFT energy.  $E_{\text{tot}}(\text{S}_8)$  represents an average energy for a typical S<sub>8</sub> molecule. Additionally, with the above definition for the formation energy, we assume that the reaction always takes place with the elemental sulfur, S<sub>8</sub>, as suggested experimentally for inverse vulcanization.<sup>[16]</sup> The formation energy defined in Eq. 3 is considered here as a measure for thermodynamic stability of DIB-S<sub>n</sub>-DIB structures with respect to  $n = 1$ . The formation energies per sulfur atom for the lowest-energy structures are shown in Figure 5. The dashed lines in the figure which connect the data points for  $n = 1$  and  $n = 2$  are guides to the eye. The standard deviation of the  $E_{\text{form}}^{(c,n)}$  calculated for the ten structures for each  $(c, n)$  are displayed in the figure as error bars. For all connections  $c$ , the sulfur chains with  $n > 1$  show lower formation energies than  $n = 1$ . Moreover, shorter sulfur chains ( $2 < n < 4$ ) are found to be somewhat more favorable, in agreement with the results in Figures 3 and 4. In this range, all connections show comparable formation energies. However, DIB-S<sub>n</sub>-DIB structures where the sulfur chain connects to the quaternary carbons of DIBs ( $c = \text{AA}$ ) exhibit slightly lower formation energies. To further validate the results in Figure 5, we additionally re-optimize DIB-S<sub>n</sub>-DIB structures with AB connection through temperature-assisted minimum-energy search at an elevated temperature, namely 500 K. The minimum-energy structure is again found to be the one with  $n = 3$  confirming the previous results above.

## 4. Conclusions

In summary, we have used density-functional theory calculation to study the local bonding between sulfur chains and the

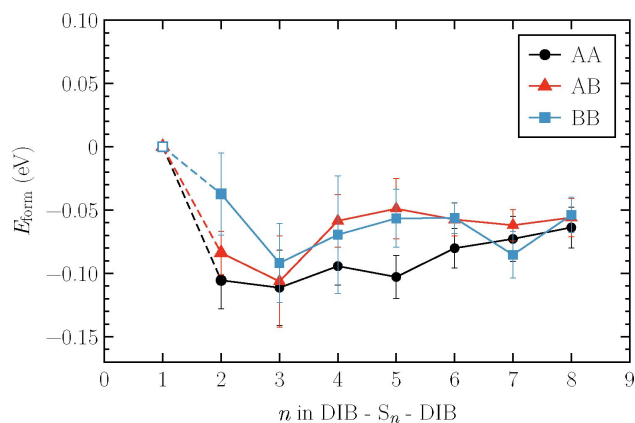


**Figure 5.** The formation energies of DIB-S<sub>n</sub>-DIB systems with different connections between the sulfur chain and the DIBs. The data points correspond to the formation energies calculated for the lowest-energy structures obtained after the simulated quenching. The error bars are the standard deviations of the formation energies calculated for all 10 uncorrelated snapshots taken from the classical MD trajectories. The dashed lines connecting the curves to the corresponding reference points,  $n = 1$ , serve as guides to the eye.

organic moieties in sulfur/1,3-diisopropenylbenzene co-polymers. We find that sulfur chains with 4 atoms are more likely to form between the diisopropenylbenzenes. We also find that the stabilization of the sulfur/1,3-diisopropenylbenzene co-polymers is brought about by the sulfur chains connecting the diisopropenylbenzene molecules and forming the polymer network. Therefore, based on our investigations, we could anticipate that the short sulfur chain with 4 atoms should also be favorable in any other sulfur/carbon co-polymers with comparable structures. We have also observed that the connection of the sulfur chain to the different carbon types in the isopropenyl groups does not have any noticeable preference.

Based on our findings on their local structure, we have shown that a thermodynamically preferred structure of a sulfur/1,3-diisopropenylbenzene co-polymer should contain about 38 wt % diisopropenylbenzene. This means that even compounds with lower organic mass fraction, which has been experimentally demonstrated to have a better electrochemical performance as cathode materials for lithium-sulfur batteries, would show a tendency towards the above-mentioned mass fraction and shorter sulfur chains after cycling. This, in turn, could mean that despite a lower cathode capacity, the sulfur/1,3-diisopropenylbenzene co-polymers with around 38 wt % of diisopropenylbenzene could maintain their capacity over a larger cycle numbers. Besides, a considerable amount of mass fraction of the carbon material could, in principle, enhance the electrical conductivity of the cathode.

## Acknowledgement

The authors gratefully acknowledge DFG funding via projects PA3141/3-1 (Project number 420536636) and PA3141/5-1 (Project number 446879138). This research was also financially supported by the European Social Funds (ESF) and the State of Saxony-Anhalt through the graduate school AgriPoly. The computations have been mostly performed on a Bull Cluster at the Center for Information Services and High Performance Computing (ZIH) at TU Dresden via the project 'p\_oligothiophenes'. Open Access funding enabled and organized by Projekt DEAL.

## Conflict of Interest

The authors declare no conflict of interest.

**Keywords:** Li–S batteries · sulfur cathodes · polymers · molecular dynamics · density functional calculations

- [1] P. G. Bruce, S. A. Freunberger, L. J. Hardwick, J.-M. Tarascon, *Nat. Mater.* **2012**, *11*(1), 19–29.
- [2] X. Ji, L. F. Nazar, *J. Mater. Chem.* **2010**, *20*(44), 9821–9826.
- [3] G. Bieker, V. Küpers, M. Kolek, M. Winter, *Commun. Mater.* **2021**, *2*(1), 1–12.
- [4] Y. V. Mikhaylik, J. R. Akridge, *J. Electrochem. Soc.* **2004**, *151*(11), A1969.
- [5] D. Moy, A. Manivannan, S. R. Narayanan, *J. Electrochem. Soc.* **2015**, *162*(1), A1.
- [6] Y. Yang, G. Zheng, Y. Cui, *Chem. Soc. Rev.* **2013**, *42*(7), 3018–3032.
- [7] M. Lécuyer, J. Gaubicher, M. Deschamps, B. Lestriez, T. Brousse, D. Guyomard, *J. Power Sources* **2013**, *241*, 249–254.
- [8] K. Jeddi, M. Ghaznavi, P. Chen, *J. Mater. Chem. A* **2013**, *1*(8), 2769–2772.
- [9] W. J. Chung, J. J. Griebel, E. T. Kim, H. Yoon, A. G. Simmonds, H. J. Ji, P. T. Dirlam, R. S. Glass, J. J. Wie, N. A. Nguyen, et al., *Nat. Chem.* **2013**, *5*(6), 518–524.
- [10] G. Li, W. Cai, B. Liu, Z. Li, *J. Power Sources* **2015**, *294*, 187–192.
- [11] J. Zhu, P. Zhu, C. Yan, X. Dong, X. Zhang, *Prog. Polym. Sci.* **2019**, *90*, 118–163.
- [12] Y. Yang, G. Yu, J. J. Cha, H. Wu, M. Vosgueritchian, Y. Yao, Z. Bao, Y. Cui, *ACS Nano* **2011**, *5*(11), 9187–9193.
- [13] S. Tu, X. Chen, X. Zhao, M. Cheng, P. Xiong, Y. He, Q. Zhang, Y. Xu, *Adv. Mater.* **2018**, *30*(45), 1804581.
- [14] C.-J. Huang, J.-H. Cheng, W.-N. Su, P. Partovi-Azar, L.-Y. Kuo, M.-C. Tsai, M.-H. Lin, S. P. Jand, T.-S. Chan, N.-L. Wu, et al., *J. Power Sources* **2021**, *492*, 229508.
- [15] P. Partovi-Azar, S. Panahian Jand, P. Kaghazchi, *Phys. Rev. Appl.* **2018**, *9*(1), 014012.
- [16] A. G. Simmonds, J. J. Griebel, J. Park, K. R. Kim, W. J. Chung, V. P. Oleshko, J. Kim, E. T. Kim, R. S. Glass, C. L. Soles, et al., *ACS Macro Lett.* **2014**, *3*(3), 229–232.
- [17] A. Hoeffling, D. T. Nguyen, P. Partovi-Azar, D. Sebastiani, P. Theato, S.-W. Song, Y. J. Lee, *Chem. Mater.* **2018**, *30*(9), 2915–2923.
- [18] T. D. Kühne, M. Iannuzzi, M. D. Ben, V. V. Rybkin, P. Seewald, F. Stein, T. Laino, R. Z. Khaliullin, O. Schütt, F. Schiffmann, et al., *J. Chem. Phys.* **2020**, *152*(19), 194103.
- [19] J. VandeVondele, J. Hutter, *J. Chem. Phys.* **2007**, *127*(11), 114105.
- [20] M. Krack, *Theor. Chem. Acc.* **2005**, *114*(1), 145–152.
- [21] J. P. Perdew, K. Burke, M. Ernzerhof, *Phys. Rev. Lett.* **1996**, *77*(18), 3865.
- [22] E. S. Zijlstra, N. Huntemann, A. Kalitsov, M. E. Garcia, U. V. Barth, *Model. Simul. Mater. Sci. Eng.* **2008**, *17*(1), 015009.
- [23] S. Grimme, J. Antony, S. Ehrlich, H. Krieg, *J. Chem. Phys.* **2010**, *132*(15), 154104.
- [24] J. Wang, R. M. Wolf, J. W. Caldwell, P. A. Kollman, D. A. Case, *J. Comput. Chem.* **2004**, *25*(9), 1157–1174.
- [25] J. D. Gale, *Philos. Mag. B* **1996**, *73*(1), 3–19.
- [26] J. D. Gale, *J. Chem. Soc. Faraday Trans.* **1997**, *93*(4), 629–637.
- [27] J. D. Gale, A. L. Rohl, *Mol. Simul.* **2003**, *29*(5), 291–341.
- [28] C. I. Bayly, P. Cieplak, W. Cornell, P. A. Kollman, *J. Phys. Chem.* **1993**, *97*(40), 10269–10280.
- [29] D. Golze, J. Hutter, M. Iannuzzi, *Phys. Chem. Chem. Phys.* **2015**, *17*(22), 14307–14316.
- [30] C. Campañá, B. Mussard, T. K. Woo, *J. Chem. Theory Comput.* **2009**, *5*(10), 2866–2878.
- [31] S. Nosé, *J. Chem. Phys.* **1984**, *81*(1), 511–519.
- [32] W. G. Hoover, *Phys. Rev. A* **1985**, *31*(3), 1695.

Manuscript received: July 8, 2021

Revised manuscript received: September 13, 2021

Accepted manuscript online: September 29, 2021

Version of record online: October 22, 2021